



VLBI astrometry

Probing astrophysics, celestial reference frames, and General Relativity

N. Bartel

York University, Department of Physics and Astronomy, 4700 Keele Street, Toronto, Ontario M3J 1P3 Canada, e-mail: bartel@yorku.ca

Abstract. We review particular achievements in VLBI astrometry that pertain to astrophysical processes in the core region of active galactic nuclei (AGN), the stability of celestial reference frames, and a test of general relativity. M81*, the core-jet source in the center of the nearby galaxy M81, was imaged at several epochs and frequencies. The least jittery part of its structure occurs at its southwesterly end, exactly where the high-frequency emission is emanating from. Since all images are phase-referenced to a largely stable and frequency independent physically unrelated source, this result is one of the strongest support for high-frequency emission originating closest to the gravitational center of the AGN. The “core” of the superluminal quasar, 3C 454.3, was used as the ultimate reference for the NASA-Stanford spaceborne relativity mission Gravity Probe B (GP-B). The core jitters along the jet direction somewhat, likely due to jet activity close to the putative supermassive black hole nearby, but is on average stationary within $39 \mu\text{as yr}^{-1}$ and $30 \mu\text{as yr}^{-1}$ in α and δ , respectively, relative to a celestial reference frame closely linked to the ICRF2. Two nearby reference sources, B2250+194 and B2252+172, were stationary with respect to each other within even smaller limits. These results indicate the degree of stability of celestial reference frames defined by extragalactic sources. The GP-B guide star, IM Pegasi, has a proper motion of $-20.83 \pm 0.09 \text{ mas yr}^{-1}$ and $-27.27 \pm 0.09 \text{ mas yr}^{-1}$ in α and δ , respectively, and a parallax of $10.37 \pm 0.07 \text{ mas}$. IM Pegasi’s radio emission originates preferentially in the polar regions relatively close to the surface of the primary of the binary system.

Key words. astrometry – techniques: interferometric – radio continuum: stars – galaxies: nuclei – galaxies: individual (M81) – relativity – stars: activity – stars: individual (IM Pegasi)

1. Introduction

Since the first phase-referenced VLBI observations were made in 1971 of the superluminal quasar 3C 345 and the quasar NRAO 512 nearby on the sky (Shapiro et al. 1979), high precision VLBI astrometry has had an impact on many areas of astrophysics, astrome-

try, physics, geophysics, and spacecraft navigation. Here we will focus on examples in three areas and point out aspects that could be relevant for the Gaia mission: 1) Astrophysics of the core region of AGN – where is the supermassive black hole, the gravitational center of the galaxy? 2) Extragalactic reference frames

– how stable are they? 3) Test of general relativity – what support did VLBI provide for Gravity Probe B (GP-B)?

2. Locating the “core” in the nuclear region of a galaxy

The region close to the putative supermassive black hole in the nuclear region of a galaxy or quasar is expected to be optically thick at radio wavelengths with the opacity decreasing along the jet axis with increasing distance from the center of activity. The position of components in the core-jet brightness distribution is influenced by this effect as first observed for the quasar pair 1038+528 A, B (Marcaide & Shapiro 1984). The most recent studies of opacity effects were made for many sources by measuring the position of the “core” component relative to an optically thin jet component in the same source at different frequencies (Kovalev et al. 2008; Sokolovsky et al. 2011). The most extensive opacity studies for a single source were made by (Bietenholz et al. 2000, 2004). These authors made measurements of the core-jet source, M81*, in the nuclear region of M81 and determined the position of the peak of the brightness distribution at several frequencies and 20 epochs relative to an unrelated outside reference point, the center of the expanding shell of supernova 1993J likely identical to the explosion center of the star and therefore sufficiently stable in frequency and time. These studies are important for mainly three reasons and are distinguished from the other studies mentioned above. First, M81, at a distance of 3.96 ± 0.29 kpc (Bartel et al. 2007), harbors the nearest extragalactic active galactic nucleus (AGN) besides Cen A at about the same distance. Activity close to the supermassive black hole can therefore be studied with high linear resolution at the distance of the source. Second, M81* is, despite its somewhat elongated shape, rather compact. A typical core-jet structure is not clearly apparent. In particular, an optically thin jet component is not clearly discernible with respect to which opacity effects in the core region could be studied. Compact sources such as M81* are however important as defining sources for ce-

lestial reference frames such as the ICRF (Ma et al. 1998) or the ICRF2 (Ma et al. 2009) that can then later be compared with the optical celestial reference frame to be defined by GAIA. Third, the investigations of M81* have been the only ones with the objective of locating the core, or the emission region closest to the supermassive black hole, by probing not only the frequency dependence of particular structural positions but also their time dependence.

Figure 1 shows the galaxy M81 in the optical as well as in the radio, with the nuclear region containing the rather compact but somewhat elongated core-jet radio source M81*. Figure 2 shows the 50% contour of the average over many epochs of an elliptical Gaussian fit to the brightness distribution of M81* at five frequencies. Clearly, the Gaussians at higher frequencies are located closer to the southwest end of the core-jet source, indicating increasing opacity toward that end. The position of the Gaussian extrapolated for $\nu \rightarrow \infty$ is close to the southwest end of the 14.8 GHz ellipse.

A further study was done to measure the jitter of the positions of different points in the brightness distribution of M81* at one frequency, 8.4 GHz (Bietenholz et al. 2000). For this purpose, the brightness distribution was fit with an elliptical Gaussian and a point source, the latter to represent the tip of the short jet. In Figure 3 the position distributions are shown for the point source, the elliptical Gaussian, and the southwestern end of the 50% contour of the elliptical Gaussian. The point source jitters most, indicating best the activity of the jet. The rms of the position values is $600 \mu\text{as}$. The rms of the position values decreases along the core-jet axis toward the southwest and reaches a minimum of $58 \mu\text{as}$ at the position indicated by the cross, almost identical to the position of the Gaussians extrapolated to $\nu \rightarrow \infty$ (see Figure 2).

The proper motion of SN 1993J relative to the core of M81* is indicated in Figure 1. It is not significant. The standard error is $9 \mu\text{as yr}^{-1}$ corresponding to 160 km s^{-1} (Bietenholz et al. 2001). It is among the lowest in astrometry and indicates the potential of VLBI (see Reid et al. (2009) for similar astrometric measurements in our own Galaxy).

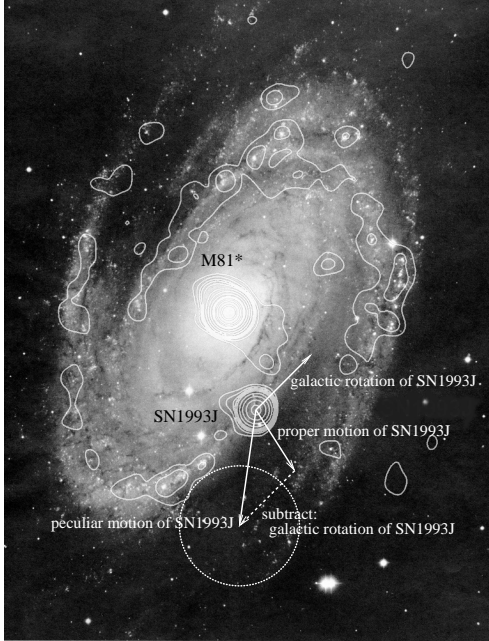


Fig. 1. Optical image of M81 with a contoured radio image at 5 GHz. The strong radio source in the center is M81*. The vectors show motion of SN 1993J, 160 arcsec south of M81*, relative to the core of M81*, with the circle representing the standard error (Bietenholz et al. 2001). Here and hereafter, north is up and east to the left.

3. Limits on the proper motion of extragalactic sources

The most fundamental reference frame in astrometry has been defined now for more than a dozen years not by optical sources but rather by radio source. The International Celestial Reference Frames, ICRF and ICRF2, are defined by compact extragalactic radio sources, the cores of radio galaxies and quasars which are routinely monitored with VLBI. Each of these sources could exhibit activity similar to typical core-jet sources even if they appear to be compact as in the case of M81*. Such activity could lead to structure changes and a proper motion of the brightness peak. Measuring the proper motion, or limits of it, of compact extragalactic radio sources is therefore important for probing the stability of celestial reference

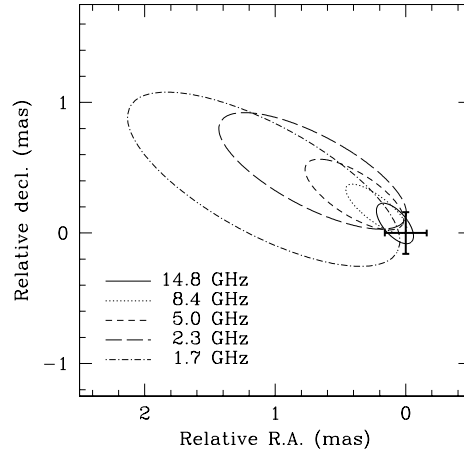


Fig. 2. The 50% contours of the average over many epochs of the elliptical Gaussians fitted to the elongated structure of M81* at each frequency. The positions of the Gaussians are determined relative to the geometric center of SN 1993J (Bietenholz et al. 2004). The position extrapolated for $\nu \rightarrow \infty$ is close to the southwest side of the 14.8 GHz ellipse and also close to the core position (cross) from Figure 3.

frames defined by such sources and for later comparisons with such reference frames defined by Gaia.

An early study led to the determination of a limit on the proper motion of two quasars, 3C 345 and NRAO 512, nearby on the sky. It was found that the core of 3C 345 was stationary relative to NRAO 512 within 1σ limits of $20 \mu\text{as yr}^{-1}$ in α and $50 \mu\text{as yr}^{-1}$ in δ (Bartel et al. 1986). Further limits were obtained, e.g., for the quasar pair 1038+528 A, B of $10 \mu\text{as yr}^{-1}$ (Rioja & Porcas 2000) and recently for four sources of $20 \mu\text{as yr}^{-1}$ in α and $30 \mu\text{as yr}^{-1}$ in δ (Fomalont et al. 2011).

Another study was made for the VLBI support (Shapiro et al. 2012) of the NASA/Stanford spaceborne relativity mission, GP-B (see, § 4). In this study the coordinates of the “core” of the superluminal quasar, 3C 454.3, were determined relative to those of the brightness peaks of two other extragalactic sources, B2250+194 and B2252+172, nearby on the sky, and also within a celestial reference

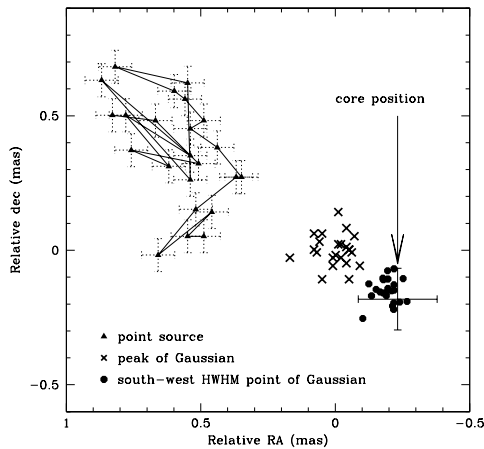


Fig. 3. Positions at each of 20 epochs over 4.5 years of three points in the two-component model as indicated, plotted with respect to the geometric center of SN 1993J. The jittery motion of the point-source (jet) is emphasized by the connecting line starting in time at the lower end. The rms of the scatter of the positions decreases toward the southwest, reaching a minimum at the “core position” (Bietenholz et al. 2000).

frame (CRF) defined by ~ 4000 compact extragalactic radio sources and almost identical to the ICRF2. The measurements are based on VLBI observations at 8.4 GHz at 35 epochs between 1997 and 2005. The source, 3C 454.3, is shown in Figures 4. As is well known, the quasar 3C 454.3 exhibits a complex bright region in the east with two strong components, C1 and C2, and a modulated extending region with several components, D1, D2, J1, and J_{ext} directed toward the northwest. The two other sources are compact and not shown here.

For the time from 2002 to 2005 for which data for B2252+172 were obtained, it was found that B2250+194 and B2252+172 are stationary relative to each other and also in the CRF within 1σ upper limits of 15 and $30 \mu\text{as yr}^{-1}$ in α and δ , respectively. The component, C1, dubbed to be the “core” at 8.4 GHz, is stationary in the CRF within 1σ upper limits of $39 \mu\text{as yr}^{-1}$ and $30 \mu\text{as yr}^{-1}$ in α and δ , respectively. These limits correspond to

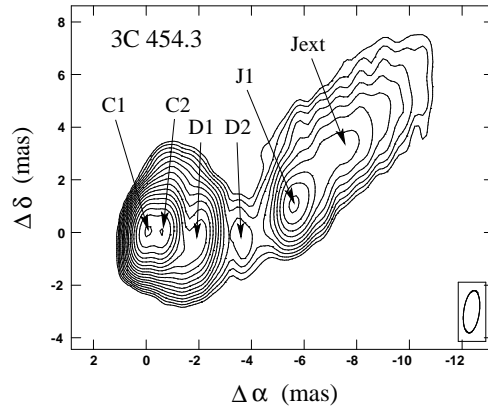


Fig. 4. An image of 3C 454.3 from observations at 8.4 GHz on 2005 May 28 with components indicated. The contours start at 10 mJy bm^{-1} and increase by factors of $\sqrt{2}$ towards the peak. The peak brightness is 2.68 Jy bm^{-1} . Here and hereafter, the full-width at half-maximum (FWHM) contour of the Gaussian convolving beam is given in a lower corner (Bartel et al. 2012).

speeds of $1.0 c$ and $0.8 c$, respectively. In contrast, some of the other components have superluminal speeds in the CRF of up to $5 c$.

Over the course of years, there is some evidence that the apparent position of the core varies over $\sim 0.2 \text{ mas}$ in α in a jittery fashion. This apparent motion could be due to slight changes in the brightness distribution around C1 caused by activity of the jet closest to the supermassive black hole in the center of 3C 454.3 (Bartel et al. 2012).

4. Astrometry of IM Pegasi, the guide star for GP-B

The NASA/Stanford GP-B mission (Everitt et al. 2011) is a relativity experiment with four superconducting gyroscopes in a satellite in a low altitude polar orbit around Earth. The experiment successfully tested two predictions of general relativity: the geodetic effect and the much smaller frame-dragging or gyromagnetic, or Lense Thirring effect, each of these two effects inducing precessions of the gyroscopes in planes perpendicular to each other.

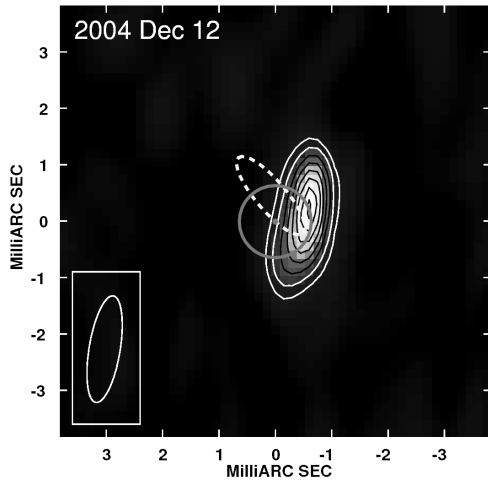


Fig. 5. An image of IM Pegasi at 8.4 GHz at the indicated epoch. The contours are drawn at 10, 20, 30, ..., 80, 90, and 98% of the peak brightness. The circle indicates the primary's optical disk and the ellipse its binary orbit (Bietenholz et al. 2012).

The geodetic effect is due to Earth's mass and is predicted to cause a precession of $6.6 \text{ arcsec yr}^{-1}$. The frame-dragging effect is due to Earth's angular momentum and is predicted to cause a precession of 39 mas yr^{-1} . GP-B was designed to measure each effect with a standard error of $\leq 0.5 \text{ mas yr}^{-1}$ relative to the distant universe. Technical limitations prevented the spacecraft from measuring the effects directly but only to an optically sufficiently bright star, the guide star for GP-B chosen to be IM Pegasi (HR8704). IM Pegasi is a close binary RS CVn with an orbital period of 24.65 d and an essentially circular orbit. The primary is a magnetically active K2 III star (Berdyugina et al. 1999; Lebach et al. 1999) and the secondary is sun-like. The star's motion needed to be determined separately, relative to the distant universe, represented by extragalactic sources.

VLBI observations were made at 8.4 GHz at 35 epochs from 1997 to 2005 to determine the position at epoch, proper motion, parallax, orbital motion, and the distribution of the locations of the star's peak emission relative to the optical disk of the star. Figure 5 shows a radio image of the star.

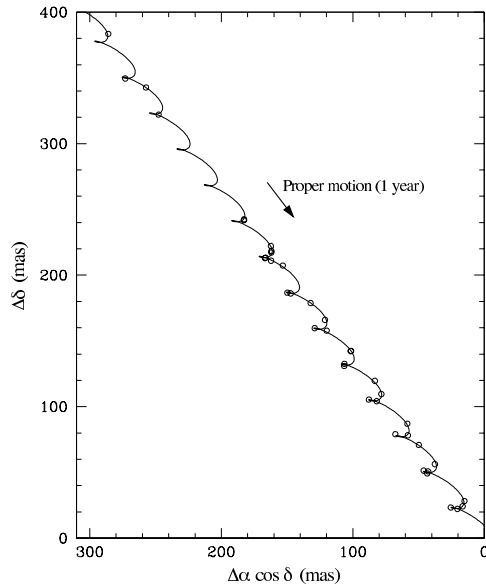


Fig. 6. Relative positions of IM Pegasi with the astrometric fit curve (Ratner et al. 2012).

The radio emission from the star is not point-like but is somewhat extended. Gaussian fits to the brightness distribution were made to obtain a representative value for the position of the star. Figure 6 shows the 35 positions of IM Pegasi and in addition four positions determined earlier, between 1991 and 1994 by Lestrade et al. (1995) in support of the Hipparcos mission. The plotted curve shows the astrometric fit. The proper motion with standard error of IM Pegasi in the CRF, almost identical to the ICRF2 as discussed in § 3, is $-20.83 \pm 0.09 \text{ mas yr}^{-1}$ and $-27.27 \pm 0.09 \text{ mas yr}^{-1}$ in α and δ , respectively. The parallax and distance with standard errors are: $10.37 \pm 0.07 \text{ mas}$ and $96.4 \pm 0.7 \text{ pc}$, respectively (Ratner et al. 2012).

In Figure 7 the positions are plotted after subtraction of the estimated position at epoch, proper motion, and parallax. The orbit of IM Pegasi is derived from the astrometric fit and also plotted in the figure. The whole picture of the binary system as seen from Earth is given in Figure 8.

In Figure 9 (left panel) the distribution of the positions of the radio emission, after further

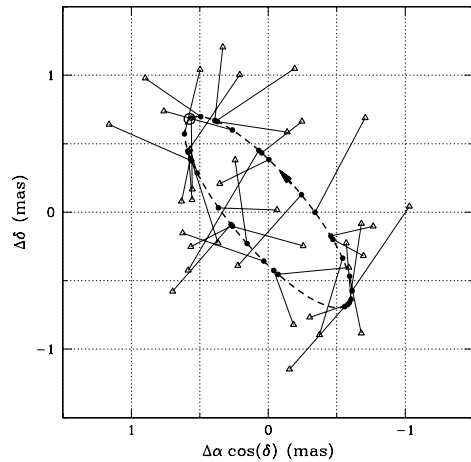


Fig. 7. Relative positions (triangles) of IM Pegasi after subtraction of the position at epoch, proper motion and parallax. Circles at inner the end of the lines give predicted positions on the fit orbit ellipse (Ransom et al. 2012).

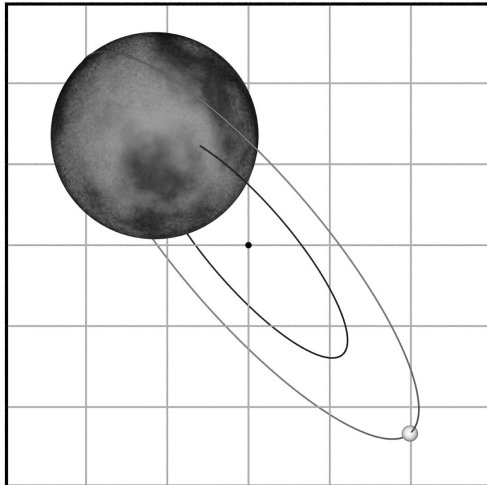


Fig. 8. Artist rendition of the primary and the secondary with orbit ellipses as seen from Earth. Grid lines are separated by 0.5 mas (Ransom et al. 2012).

subtraction of the orbit, are plotted, together with the optical disk of the primary. Almost certainly, the active primary is the source of the radio emission of IM Pegasi. After the Algol system (Lestrade et al. 1993), this is the second

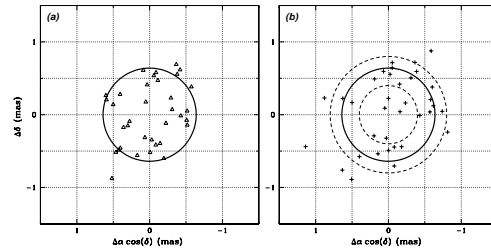


Fig. 9. (a) The distribution of the observed positions (centers of fit Gaussians) of IM Pegasi after removal of the estimated orbit together with the optical disk of the primary. (b) As in (a) but now for the brightness-peak positions. The dashed circles are used for counting analysis (Ransom et al. 2012).

close binary system for which such an identification could be made. The locations of highest activity are better given by the positions of the brightness peaks as shown in the right panel. These positions are scattered across the disk of the primary but not much beyond. In fact simulations show that most of the emission peaks occur close to the star's surface with $\sim 2/3$ of them at altitudes not higher than 25% of the radius of the primary. Further, the emission peaks occur preferentially along an axis closely aligned with the spin axis of the primary expected to be parallel to the orbit normal. In particular, simulations suggest that the emission peaks occur $3.6^{+0.4}_{-0.7}$ times more frequently near the pole regions at latitudes $\geq 70^\circ$ than near the equator at latitudes $\leq 20^\circ$ (Ransom et al. 2012). This dependence on latitude is similar to that found for the occurrence of the optical active regions seen as dark spots with Doppler imaging (Berdyugina & Marsden 2006).

The VLBI astrometry support for GP-B was the determination of the proper motion of IM Pegasi. The final experimental results of GP-B are measurements of the weighted average precession of all four gyroscopes due to the geodetic effect of $-6,501.8 \pm 18.3 \text{ mas yr}^{-1}$ and due to the frame-dragging effect of $-37.2 \pm 7.2 \text{ mas yr}^{-1}$, confirming the predictions of general relativity (Everitt et al. 2011).

5. Conclusions

1. Finding the “core,” the radio emission region closest to the putative supermassive black hole in a galaxy or quasar is an important goal for studying astrophysics of core-jet sources and the stability of celestial reference frames defined by extragalactic radio sources. The compact core-jet source, M81* in the center of the galaxy M81, was the subject of extensive studies of opacity effects along the core-jet axis and of locating the core. The core position was identified 1) in frequency as the point of peak emission for $\nu \rightarrow \infty$ and 2) in time as the least jittery or most stable point in the structure of M81*.
2. The stability of an extragalactic reference frame closely related to the ICRF2 was probed. The core of 3C 454.3 has no significant proper motion in that frame with 1σ upper limits of $39 \mu\text{as yr}^{-1}$ and $30 \mu\text{as yr}^{-1}$ in α and δ , respectively.
3. IM Pegasi’s proper motion and parallax were determined for the support of GP-B. Radio emission emanates from the primary, preferentially in the polar region and close to the surface of the star.

References

- Bartel, N., et al. 1986, *Nature*, 319, 733
- Bartel, N., Bietenholz, M. F., Rupen, M. P., & Dwarkadas, V. V. 2007, *ApJ*, 668, 924
- Bartel, N., et al. 2012, *ApJS*, in press
- Berdyugina, S. V., Ilyin, I., & Tuominen, I. 1999, *A&A*, 347, 932
- Berdyugina, S. V., & Marsden, S. C. 2006, in *ASP Conf. Series*, Vol. 358, 385
- Bietenholz, M. F., Bartel, N., & Rupen, M. P. 2000, *ApJ*, 532, 895
- Bietenholz, M. F., Bartel, N., & Rupen, M. P. 2001, *ApJ*, 557, 770
- Bietenholz, M. F., Bartel, N., & Rupen, M. P. 2004, *ApJ*, 615, 173
- Bietenholz, M. F., et al. 2012, *ApJS*, in press
- Everitt, C. W. F. et al. 2011, *Phys. Rev. Lett.*, 106, 221101, 1105.3456
- Fomalont, E., et al. 2011, *AJ*, 141, 91
- Kovalev, Y. Y., Lobanov, A. P., Pushkarev, A. B., & Zensus, J. A. 2008, *A&A*, 483, 759
- Lebach, D. E., et al. 1999, *ApJ*, 517, L43
- Lestrade, J.-F., Phillips, R. B., Hodges, M. W., & Preston, R. A. 1993, *ApJ*, 410, 808
- Lestrade, J.-F., Jones, D. L., Preston, R. A., et al. 1995, *A&A*, 304, 182
- Ma, C., et al. 1998, *AJ*, 116, 516
- Ma, C., Arias, et al. 2009, *IERS Technical Note*, 35, 1
- Marcaide, J. M., & Shapiro, I. I. 1984, *ApJ*, 276, 56
- Ransom, R. R., et al. 2012, *ApJS*, in press
- Ratner, M. I., et al. 2012, *ApJS*, in press
- Reid, M. J., et al. 2009, *ApJ*, 700, 137
- Rioja, M. J., & Porcas, R. W. 2000, *A&A*, 355, 552
- Shapiro, I. I., Wittels, J. J., et al. 1979, *AJ*, 84, 1459
- Shapiro, I. I., et al. 2012, *ApJS*, in press
- Sokolovsky, K. V., Kovalev, Y. Y., Pushkarev, A. B., & Lobanov, A. P. 2011, *A&A*, 532, A38